Tuning the Photoluminescence of Graphene Quantum Dots through the Charge Transfer Effect of Functional Groups

Sung Hwan Jin,[†] Da Hye Kim,[‡] Gwang Hoon Jun,[†] Soon Hyung Hong,[†] and Seokwoo Jeon[†,*]

[†]Department of Material Science & Engineering, Graphene Research Center (GRC), KAIST Institute for the Nanocentury, Korea Advanced Institute of Science and Technology (KAIST), 291 Daehak-ro, Yuseong-gu, Daejeon 305-701, Korea and [‡]Korea Institute of Industrial Technology, 711 Hosan-dong, Dalseo-gu, Daegu 704-203, Korea

ABSTRACT The band gap properties of graphene quantum dots (GQDs) arise from quantum confinement effects and differ from those in semimetallic graphene sheets. Tailoring the size of the band gap and understanding the band gap tuning mechanism are essential for the applications of GQDs in opto-electronics. In this study, we observe that the photoluminescence (PL) of the GQDs shifts due to charge transfers between functional groups and GQDs. GQDs that are functionalized with amine groups and are 1−3 layers thick and less than 5 nm in diameter were successfully fabricated using a two-step cutting process from graphene oxides (GOs). The functionalized GQDs exhibit a redshift of PL emission (*ca.* 30 nm) compared to the unfunctionalized GQDs. Furthermore, the PL emissions of the GQDs and the amine-functionalized GQDs were also shifted by changes in the pH due to the protonation or deprotonation of the functional groups. The PL shifts resulted from charge transfers between the functional groups and GQDs, which can tune the band gap of the GQDs. Calculations from density functional theory (DFT) are in good agreement with our proposed mechanism for band gap tuning in the GQDs through the use of functionalization.

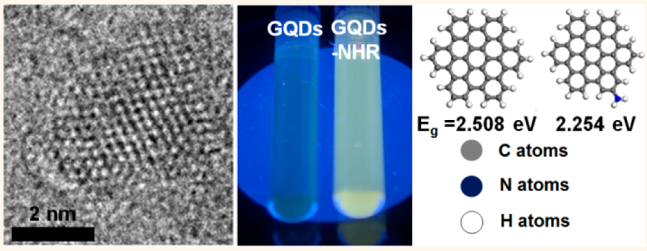

KEYWORDS: graphene quantum dots · photoluminescence · functionalization · density functional theory · band gap

Recently, zero-dimensional graphene quantum dots (GQDs) have received considerable attention as a new type of quantum dot because of their unique electronic and opto-electronic properties. Unlike two-dimensional graphene, GQDs have a band gap because of quantum confinement[1−3] and exhibit strong photoluminescence (PL).[4−7] Some studies have demonstrated the possibility of tailoring the band gap or PL emission of GQDs. In principle, the band gap of GQDs is highly influenced by their size due to the quantum confinement effect that highlights when their diameter is less than 10 nm. Ritter *et al.*[8] and Lu *et al.*[9] demonstrated the size dependence of the GQDs' band gap using scanning tunneling spectroscopy experiments. These authors clearly demonstrated that the band gap of the GQDs increases as the size of the GQDs decreases. Peng *et al.*[10] also reported that the PL emission of the GQDs is blueshifted when their size is decreased because of the increased band gap of the GQDs. Another route to tune the band gap of GQDs is through chemical functionalization. Gupta *et al.*[11] demonstrated that the PL emission from the GQDs was shifted by functionalizing the GQDs, but the underlying mechanism of the shift was unclear. Zhu *et al.*[12] also reported that the PL shift resulting from the chemical functionalization can be explained by suppression of the defect state emission, thereby allowing the intrinsic state emission from the band gap of the GQDs to play a leading role in the PL emission.

Overall, the mechanism for the band gap tuning or PL shifting of the GQDs through chemical functionalization requires further study in contrast to the size-dependent band gap tuning in GQDs, which has been

* Address correspondence to jeon39@kaist.ac.kr.

Received for review October 9, 2012 and accepted December 28, 2012.

Published online December 28, 2012
10.1021/nn304675g

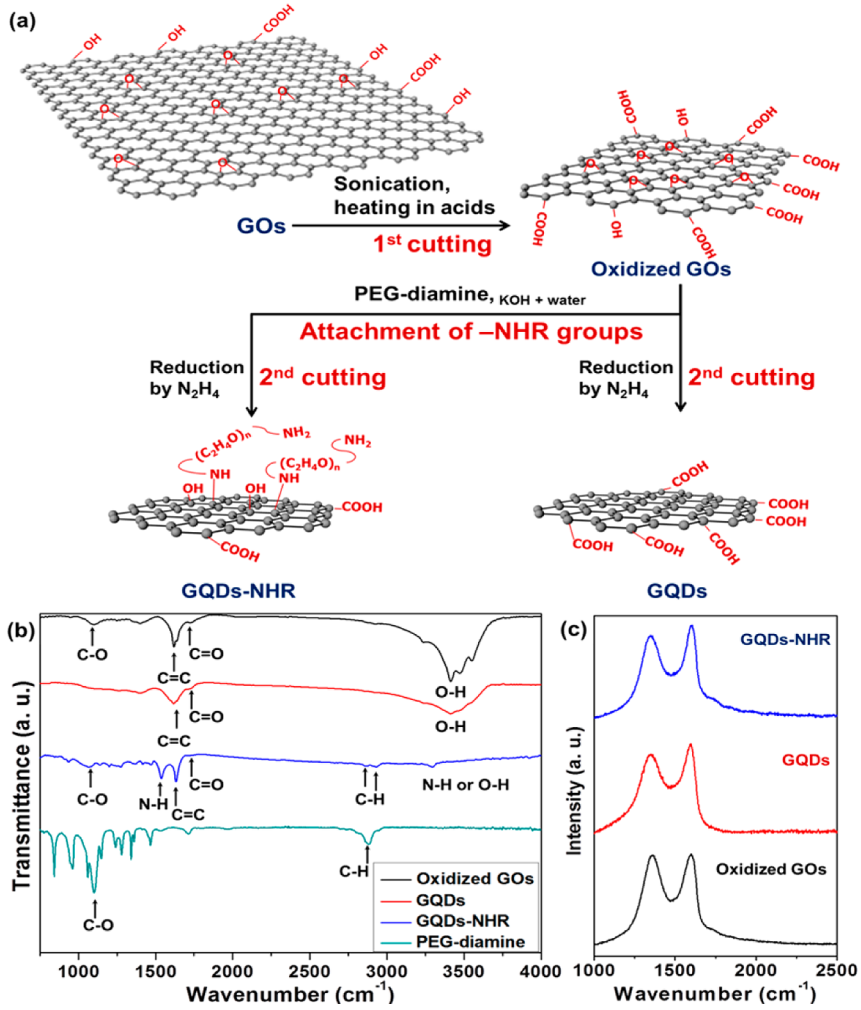

Figure 1. (a) Schematics of GQDs and GQDs-NHR from GOs, (b) FT-IR spectra, (c) Raman spectra of oxidized GOs, GQDs, and GQDs-NHR.

more thoroughly examined. Here, we report on the PL shift of GQDs through chemical functionalization and identify the mechanism for this shift. GQDs with and without amine functional groups were fabricated from the sequential oxidation and reduction of graphene oxides (GOs). The PL emission of the GQDs functionalized with amine groups exhibits a redshift compared to that of the unfunctionalized GQDs. Furthermore, the PL emissions of the GQDs and the amine group-functionalized GQDs are shifted when the pH is changed because of the protonation or deprotonation of the functional groups. The mechanism for the change in the PL emission of the GQDs by functionalization is supported by calculations based on density functional theory (DFT). From both experimental and computational analyses, the electron-withdrawing or electron-donating behaviors of the functional groups can tune the band gap of the GQDs and explain the corresponding peak shifts of the PL emission. To the best of our knowledge, this study is the first that tunes and identifies the change of the band gap in GQDs by functionalization, through the charge distribution between the GQDs and the functional groups.

RESULTS AND DISCUSSION

In this study, the GQDs and the amine group-functionalized GQDs were fabricated by cutting GOs in a two-step process, as shown in Figure 1a. First, the GOs were cut by oxidation in a mixture of H_2SO_4/HNO_3. In general, epoxy groups on the plane of the GOs are generated through the growth of epoxy chains, and they are transformed into carbonyl groups during the oxidation process, which results in the cutting of graphene.[13] Second, the sizes of the oxidized GOs were further reduced by a reduction process. During the reduction by N_2H_4, a further cutting of graphene occurred because the bridging O atoms in the remaining epoxy chains on the oxidized GOs are removed.[14] This two-step cutting process facilitated the fabrication of the GQDs. To fabricate the amine group-functionalized GQDs, oxidized GOs were reacted with diamine terminated polyethylene glycol (PEG-diamine) between the oxidation and reduction steps. Alkyl amine groups

were attached to the oxidized GOs by the ring-opening reaction of the epoxy groups on the GOs under alkali conditions,[15] which eventually formed the alkyl amine-functionalized GQDs (GQDs-NHR). A more detailed description of the fabrication of the GQDs and the GQDs-NHR is provided in the experimental methods section.

During each step of the preparation of the GQDs and the GQDs-NHR, the functional groups were identified using Fourier transform infrared (FTIR) spectroscopy, as shown in Figure 1b. The FTIR spectrum of the oxidized GOs exhibits a C−O stretching peak in ester at *ca.* 1100 cm^{-1}, a C═O stretching peak in carboxylic acid at *ca.* 1725 cm^{-1}, and broad O−H stretching peaks at *ca.* 3400 cm^{-1}. After reduction without functionalization, the GQDs exhibit a decrease in the intensity of the C−O and O−H stretching peaks due to deoxygenation. However, the C═O stretching peak in carboxylic acid remains, which originates from the carboxyl acid groups at the edge of the GQDs after reduction with N_2H_4.[16,17] In contrast to the oxidized GOs and GQDs, the GQDs-NHR exhibit new peaks at *ca.* 1536 and doublet peaks at *ca.* 2860 and 2930 cm^{-1} that correspond to N−H bending in the amine group and C−H stretching in the alkyl chains,[18,19] respectively. This result clearly shows that alkyl amine groups were attached to the GQDs. Figure 1c presents the Raman spectra of the oxidized GOs, GQDs, and the GQDs-NHR. These spectra have two typical peaks at *ca.* 1350 and 1600 cm^{-1}, which correspond to the D band and the G band of graphene, respectively. The I_D/I_G ratio of the oxidized GOs is *ca.* 0.99, which decreased to *ca.* 0.88 in the GQDs due to the reduction of the oxidized GOs. The GQDs-NHR also have an I_D/I_G ratio (*ca.* 0.89) that is similar to the GQDs, which means that the functionalization of the GQDs did not significantly affect their quality. Furthermore, the I_D/I_G ratios of our GQDs and GQDs-NHR are similar to that of GQDs produced from the oxidation of carbon fibers,[10] which may be due to the oxidative nature of the fabrication process for GQDs.

Figure 2a presents a transmission electron microscopy (TEM) image of the GQDs-NHR produced in this work. This figure reveals that *ca.* 1−5 nm sized GQDs-NHR are uniformly distributed without agglomeration. The size distribution of the GQDs-NHR is shown in Figure 2b. The average size of the GQDs-NHR is *ca.* 2.45 ± 0.63 nm, which is similar to that of the as-prepared GQDs (*ca.* 2.51 ± 0.66 nm, Supporting Information, Figure S1). The lattice spacing of the GQDs-NHR in the high resolution (HRTEM) image (Figure 2b) is *ca.* 2.143 Å, which is similar to the hexagonal pattern of graphene with d_{1100}.[20−22] Although the edges of GQDs and GQDs-NHR are irregular and unclear due to defects and functional groups, they show the random or mixed edges consisting of zigzag and armchair edges (Figure 2c and Supporting Information, Figure S1). Since the most GQDs and GQDs-NHR are close to circular shapes rather than polygonal shapes, both of them show the random or mixed edges.[6] It shows that edge structures of GQDs are not significantly affected by functionalization. Figure 2 panels d, e, and f present an atomic force microscopy (AFM) image of the GQDs-NHR on a mica substrate, the height line profile, and their height distribution, respectively. The average height of the GQDs-NHR is 1.07 ± 0.59 nm, and more than 80% of the GQDs-NHR are less than 2 nm in height. This result demonstrates that our GQDs-NHR primarily consist of 1−3 layers.[23,24] The average height of the as-prepared GQDs is 1.31 ± 0.56 nm, and the GQDs also consist of 1−3 graphene layers (Supporting Information, Figure S1). These results demonstrate that the functionalization of the GQDs does not significantly alter their microstructures, such as their size, height, and edge structures.

Figure 3a presents the PL emission spectra of the aqueous solutions of GQDs and GQDs-NHR with excitation from a 325 nm laser. The PL intensity of the GQDs-NHR is considerably greater than that of the GQDs. It has been previously reported that the surface passivation of carbon dots[25] and GQDs[11,26] with organic or polymeric species can enhance the PL emission, although surface passivation agents are nonemissive at visible wavelengths. The maximum PL position of the GQDs is *ca.* 500 nm, which is red-shifted to *ca.* 528 nm after functionalization with the alkyl amine, GQDs-NHR, as shown in normalized PL emission spectra of GQDs and GQDs-NHR (Figure 3b). The inset of Figure 3b is a photograph of aqueous solutions of the GQDs and GQDs-NHR collected under excitation with a 355 nm laser. The GQDs exhibit a bluish-green color, whereas the GQDs-NHR exhibit a more yellowish color (more detailed information is provided in Supporting Information, Figure S2). Because the sizes and heights of the GQDs and GQDs-NHR are similar, this redshift behavior primarily originates from functionalization. We hypothesize that the unpaired electrons of the amine functional groups can contribute to the electron donation from the amine groups to the GQDs based on the electron-withdrawing and electron-accepting behaviors of functional groups to benzene, which are well-known behaviors in organic chemistry.[27] Increasing the electron density can cause the lowering the band gap[28,29] of GQDs that is similar tendency to increasing the size of the GQDs, which could result in a redshift. To support this hypothesis, we observed the PL shifts while changing the pH of the GQDs and GQDs-NHR solutions. Figure 3 panels c and d present the pH-dependent PL spectra of the GQDs and GQDs-NHR, respectively. At a pH of 10, the remaining carboxylic acid group (−COOH) in the GQDs is deprotonated ($-COO^-$). The charged electron of the carboxyl groups can weaken the electron-withdrawing properties of the carboxylic acid to GQDs; consequently, the maximum PL position of the GQDs can

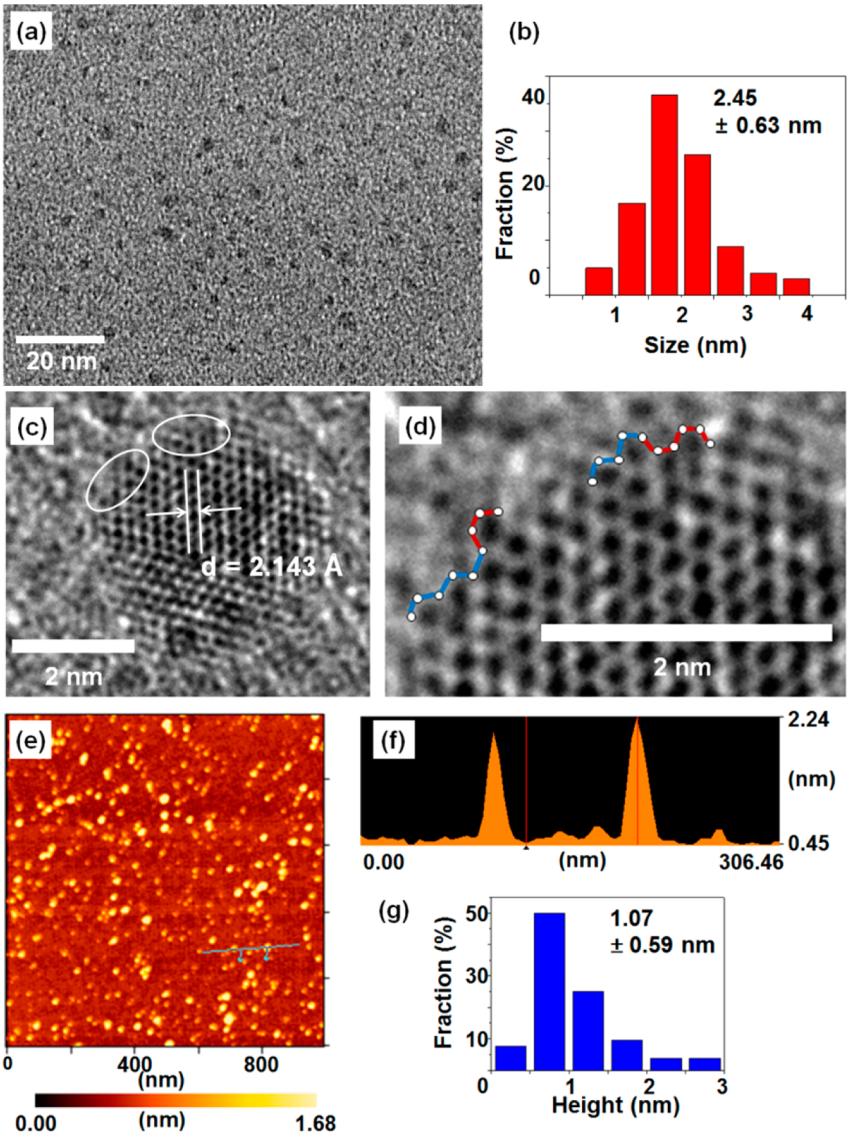

Figure 2. (a) TEM image, (b) size distribution, (c) HRTEM image with measured lattice spacing, (d) edge structures of circles in panel c (blue and red lines show zigzag and armchair edges, respectively), (e) surface height image (AFM, noncontact mode), (f) height line profile in panel e, and (g) height distribution of GQDs-NHR.

be red-shifted. However, at a pH of 1, the carboxylic acid in the GQDs is rarely protonated; the maximum PL position of the GQDs barely shifts. The GQDs-NHR presented opposite pH-dependent PL spectra to those of the GQDs. The maximum PL position of the GQDs-NHR is blueshifted at a pH of 1, and it remains similar at a pH of 10. The protonated alkyl amine group ($-NH_2^+R$) at a pH of 1 can dismiss the unpaired electrons, which act as electron donors in the amine groups. The protonated alkyl amine group can only decrease the electron density in the GQDs due to the strong electronegativity of the N atom. Alkyl amine groups are rarely deprotonated at a pH of 10; therefore, the maximum PL position of the GQDs-NHR can barely shift. These results clearly demonstrate that the PL emission of GQDs can be tuned by the charge transfer between the functional groups and GQDs. To confirm that the PL shift comes from quantum size effects, we also carefully performed a PL emission experiment on source GOs and equivalently treated, or functionalized, samples. More detailed PL spectra of those samples are presented in Supporting Information, Figures S3−S5 and clearly show different peak locations, shapes, and intensities from the measured spectra of GQD samples.

The PL shift behavior of the GQDs by functionalization was confirmed using DFT calculations (computational details are available in the computational methods section). It is known that the PL emission of GQDs originates from sp^2 clusters that are isolated within the sp^3 carbon or defects in GQDs.[30−32] We assumed that our GQDs consist of isolated sp^2 clusters within the sp^3 carbon matrix including defects like vacancies. Furthermore, we simplified the alkyl amine functional group to an amino group ($-NH_2$) at the sp^2 clusters,

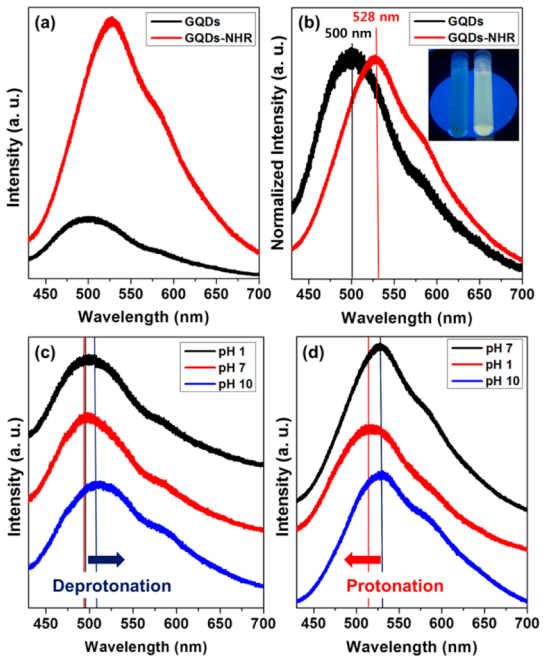

Figure 3. (a) PL, (b) normalized PL spectra of GQDs and GQDs-NHR in water (inset: photograph of GQDs (left) and GQDs-NHR (right) taken under 355 nm laser excitation); pH-dependent PL spectra of (c) GQDs and (d) GQDs-NHR.

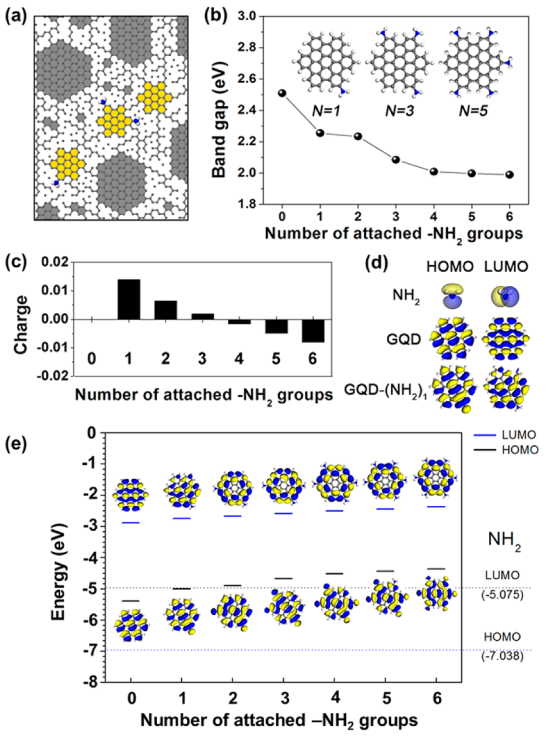

Figure 4. (a) Schematics of isolated sp^2 clusters with amino functional groups within the sp^3 carbon matrix including defects, (b) band gap change of GQD-$(NH_2)_n$ as function of the number of attached $-NH_2$ groups (inset images are optimized configuration of GQD-$(NH_2)_n$), (gray, C; white, H and blue, N atom), (c) the evolution of average Mulliken charge for amino groups as a function of the number of attached $-NH_2$ groups, (d) HOMO and LUMO isosurface of NH_2, GQD, GQD-$(NH_1)_1$, (e) HOMO and LUMO energy levels of GQDs-$(NH_2)_n$. black and blue lines indicate HOMO and LUMO levels of GQDs-$(NH_2)_n$, respectively. The dotted lines denote the HOMO and LUMO energy level of NH_2. Insets describe HOMO and LUMO isosurface of each system (the isovalue is 0.01 e/Å^3).

which consists of 13 aromatic rings (Figure 4a). The band gap of 13 aromatic rings is 2.508 eV, which is similar to the experimental data for the PL peak maximum of the GQDs (2.480 eV). Figure 4b shows the evolution of the calculated band gap of the GQDs as a function of the number of attached $-NH_2$ groups. The band gap of the GQDs decreases to 2.254 eV when a GQD is functionalized by one amino group (GQD-$(NH_2)_1$) and gradually decreases by increasing the number of $-NH_2$ groups. This behavior is related to the charge redistribution that results from functionalization. In the GQD-$(NH_2)_1$, NH_2 is positively charged due to the electron donation from the lone pair electrons of NH_2 to the antibonding state in the benzene ring, which results in the decrease of the band gap of GQD-$(NH_2)_1$. Therefore, the optimized configuration of the $-NH_2$ group in the GQD-$(NH_2)_n$ was flattened, not a pyramidal structure, as shown in the inset ($N = 1, 3, 5$) of Figure 4b. (More detailed information about the optimized configurations of GQD-$(NH_2)_n$ is provided in Supporting Information, Tables S1 and S2.) Figure 4c is the change in the average Mulliken charge for the amino groups as a function of the number of attached $-NH_2$ groups in the GQD-$(NH_2)_n$. (More detailed information on the Mulliken charge analysis of the GQD-$(NH_2)_1$ is shown in Supporting Information, Table S3.) Electron transfer from $-NH_2$ to the ring is predominant, and the average charge of the attached $-NH_2$ groups has a positive value until three $-NH_2$ groups are attached. Therefore, the band gap considerably decreases due to the increased electron density in a GQD-$(NH_2)_n$. When more $-NH_2$ groups are attached, the average charge of the attached $-NH_2$ groups has negative values and the band gaps of the GQD-$(NH_2)_n$ are saturated. In Figure 4d, the highest occupied molecular orbital (HOMO) for a GQD and the lowest occupied molecular orbital (LUMO) for NH_2 are observed in the HOMO isosurface for GQD-$(NH_2)_1$. The HOMO state for a GQD and the LUMO state for a NH_2 are in similar energy levels, and the energy level of the HOMO state for a GQD becomes gradually higher than the LUMO state for NH_2 by attaching the $-NH_2$ groups (Figure 4e). According to the increased number of attached $-NH_2$ groups, more electrons diffuse from the HOMO state to the LUMO state, and consequently from a GQD to NH_2. This electron transfer from a GQD to $-NH_2$ groups compensates the electron donation from the $-NH_2$ groups to the GQD. This compensation results in little change of the band gap of the GQD, with a greater number of attached $-NH_2$ groups.

CONCLUSION

We have experimentally demonstrated a PL shift in GQDs by functionalization and computationally identified their band tuning mechanism using DFT calculations. Both experimental and computational analyses reveal that the charge transfer between

functional groups and GQDs can tune the band gap of the GQDs, and consequently, the PL emission due to the changing electron density in the GQDs. Our research results suggest a simple route for the PL tuning of GQDs and a possible mechanism for changing the electronic band through functionalization. These results can be useful for future graphene-based optoelectronic applications.

EXPERIMENTAL AND COMPUTATIONAL METHODS

Preparation of Graphite Oxides. Graphite oxides were fabricated using the modified Hummers method.[21] An amount of 1 g of highly ordered pyrolytic graphite (SP-1, Bay Carbon Inc.) was stirred in 40 mL of concentrated H_2SO_4, which was followed by the slow addition of 3.5 g of $KMnO_4$ in an ice bath. After the addition of $KMnO_4$, the temperature was increased to 35 °C and the mixture was stirred for 2 h. Then, 150−200 mL of water was added and 5−10 mL of H_2O_2 was sequentially added dropwise into the mixture until the bubbling was finished in an ice bath. The mixture was filtered with a glass filter and washed with a 10% HCl aqueous solution. Finally, brown powders were obtained after the mixture was dried under vacuum for several days.

Preparation of Oxidized GOs, GQDs, and GQDs-NHR. Fifty milligrams of the graphite oxides was sonicated in 100 mL of a H_2SO_4/HNO_3 (volume ratio = 3:1) solution for 12 h and then refluxed at 100 °C for 24 h (1st cutting step). The suspension was centrifuged at 10000 rpm for 30 min, and dark brown precipitates were collected after the removal of acid. Then, the precipitates were sonicated in 50 mL of water and dialyzed in dialysis tubing (8000 Da, Spectrum Lab. Inc.) to adjust the pH to 7. After dialysis, an aqueous suspension of oxidized GOs was obtained. An amount of 25 mg of KOH was added to 25 mL of the oxidized GO suspension. The suspension was stirred at 80 °C for 24 h after the addition of 250 mg of PEG-diamine (average molecular weight: 3400, Sigma-Aldrich) (functionalization step). Then, 6 μL of N_2H_4 was added into the suspension, and it was stirred at 100 °C for 24 h (2nd cutting and reduction step). Finally, an aqueous suspension of the GQDs-NHR was obtained after dialysis for 7−10 days to remove the unattached PEG-diamine or remaining salts. All of the preparation steps for the GQDs are the same as for the GQDs-NHR, but it was only stirred without addition of PEG-diamine during the functionalization step.

Characterizations. FT-IR spectra were recorded using the KBr pellet method (Jasco FT/IR-4100 type-A spectrometer), and high-resolution dispersive Raman microscope results were obtained from excitation with a 325 nm laser source (LabRAM HR UV/vis/NIR). The microstructures of the GQDs and GQDs-NHR were observed with a TEM (Tecnai G2 F30 S-Twin), Cs-corrected scanning TEM (JEOL JEM-ARM200F) and AFM (Seiko). The PL spectra of an aqueous suspension in a quartz cell (path length = 5 mm) were obtained using a 325 nm laser excitation with a micro PL system (LabRAM HR UV/vis/NIR PL).

Computational Methods. The optimized equilibrium structures were calculated using density functional theory calculations with the atomic orbital-based $Dmol^3$ software package.[33] The spin-polarized Kohn−Sham equation was expanded in a local atomic orbital with the DNP basis set. The exchange correlation potential is described in terms of the PWC local density approximation (LDA). The convergence tolerances for the geometry optimization were set to 10^{-5} Ha for the energy, 0.002 Ha/Å for the force, and 0.005 Å for the displacement. The electronic SCF tolerance was 10^{-6} Ha. We considered all available configurations of GQD-$(NH_2)_n$ (n, the number of attached $-NH_2$ groups, n = 0, 1, 2, ..., 6) and determined the optimized configuration of each system by comparing the total energy. The calculated band gap was obtained from the difference between the HOMO and the LUMO. The atomic charge distribution was analyzed using the Mulliken method.[34]

Conflict of Interest: The authors declare no competing financial interest.

Supporting Information Available: Microstructure of GQDs, digital photography of GQDs aqueous solution, PL spectra of GOs and related concerns, computational details. This material is available free of charge *via* the Internet at http://pubs.acs.org.

Acknowledgment. This research was supported by the Converging Research Center Program through the National Research Foundation of Korea (NRF) funded by the Ministry of Education, Science, and Technology (2011K000623). It was also partially supported by a grant (2011-0031630) from the Center for Advanced Soft Electronics under the Global Frontier Research Program of the Ministry of Education, Science and Technology and, the GRC project of KAIST Institute for the NanoCentury. We also specially thanks to Dr. Jong Hyun Park in the LG Display R&D Center for helpful advice and discussion of optical characterization.

REFERENCES AND NOTES

1. Yan, X.; Cui, X.; Li, B.; Li, L. Large, Solution-Processable Graphene Quantum Dots as Light Absorbers for Photovoltaics. *Nano Lett.* **2010**, *10*, 1869–1873.
2. Neubeck, S.; Ponomarenko, L. A.; Freitag, F.; Giesbers, A. J. M.; Zeitler, U.; Morozov, S. V.; Blake, P.; Geim, A. K.; Novoselov, K. S. From One Electron to One Hole: Quasiparticle Counting in Graphene Quantum Dots Determined by Electrochemical and Plasma Etching. *Small* **2010**, *6*, 1469–1473.
3. Li, L.-S.; Yan, X. Colloidal Graphene Quantum Dots. *J. Phys. Chem. Lett.* **2010**, *1*, 2572–2576.
4. Li, M.; Wu, W.; Ren, W.; Cheng, H.-M.; Tang, N.; Zhong, W.; Du, Y. Synthesis and Upconversion Luminescence of N-Doped Graphene Quantum Dots. *Appl. Phys. Lett.* **2012**, *101*, 103107.
5. Liu, R.; Wu, D.; Feng, X.; Mullen, K. Bottom-Up Fabrication of Photoluminescent Graphene Quantum Dots with Uniform Morphology. *J. Am. Chem. Soc.* **2011**, *133*, 15221–15223.
6. Kim, S.; Hwang, S. W.; Kim, M. -K.; Shin, D. Y.; Shin, D. H.; Kim, C. O.; Yang, S. B.; Park., J. H.; Hwang, E.; Choi, S. −H.; *et al.* Anomalous Behaviors of Visible Luminescence from Graphene Quantum Dots: Interplay between Size and Shape. *ACS Nano* **2012**, *6*, 8203–8308.
7. Mueller., M. L.; Yan, X.; McGuire, J. A.; Li, L. Triplet States and Electronic Relaxation in Photoexcited Graphene Quantum Dots. *Nano Lett.* **2010**, *10*, 2679–2682.
8. Ritter, K. A.; Lyding, J. W. The Influence of Edge Structure on the Electronic Properties of Graphene Quantum Dots and Nanoribbons. *Nat. Mater.* **2009**, *8*, 235–242.
9. Lu, J.; Yeo, P. S. E.; Gan, C. K.; Wu, P.; Loh, K. P. Transforming C_{60} Molecules into Graphene Quantum Dots. *Nat. Nanotechnol.* **2011**, *6*, 247–252.
10. Peng, J.; Gao, W.; Gupta, B. K.; Liu, Z.; Romero-Aburto, R.; Ge, L.; Song, L.; Alemany, L. B.; Zhan, X.; Gao, G.; *et al.* Graphene Quantum Dots Derived from Carbon Fibers. *Nano Lett.* **2012**, *12*, 844–849.
11. Gupta, V.; Chaudhary, N.; Srivastava, R.; Sharma, G. D.; Bhardwaj, R.; Chand, S. Luminscent Graphene Quantum Dots for Organic Photovoltaic Devices. *J. Am. Chem. Soc.* **2011**, *133*, 9960–9963.
12. Zhu, S.; Zhang, J.; Tang, S.; Qiao, C.; Wang, L.; Wang, H.; Liu, X.; Li, B.; Li, Y.; Yu, W.; Wang, X.; Sun, H.; Yang, B. Surface Chemistry Routes to Modulate the Photoluminescence of Graphene Quantum Dots: From Fluorescence Mechanism to Up-Conversion Bioimaging Applications. *Adv. Funct. Mater.* **2012**, *22*, 4732–4740.
13. Li, Z.; Zhang, W.; Luo, Y.; Yang, J.; Hou, J. G. How Graphene Is Cut upon Oxidation? *J. Am. Chem. Soc.* **2009**, *131*, 6320–6321.

14. Pan, D.; Zhang, J.; Li, Z.; Wu, M. Hydrothermal Route for Cutting Graphene Sheets into Blue-Luminescent Graphene Quantum Dots. *Adv. Mater.* **2010**, *22*, 734–738.
15. Yang, H. F.; Shan, C. S.; Li, F. H.; Han, D. X.; Zhang, Q. X.; Niu, L. Covalent Functionalization of Polydisperse Chemically-Converted Graphene Sheets with Amine-Terminated Ionic Liquid. *Chem. Commun.* **2009**, 3880–3882.
16. Li, D.; Muller, M.; Gilje, S.; Kaner, R.; Wallace, G. Processable Aqueous Dispersions of Graphene Nanosheets. *Nat. Nanotechnol.* **2008**, *3*, 101–105.
17. Choi, E. Y.; Han, T. H.; Hong, J. H.; Kim, J. E.; Lee, S. H.; Kim, H. W.; Kim, S. O. Noncovalent Functionalization of Graphene with End-Functional Polymers. *J. Mater. Chem.* **2010**, *20*, 1907–1912.
18. Cheng, C. F.; Cheng, H. H.; Cheng, P. W.; Lee, Y. J. Effect of Reactive Channel Functional Groups and Nanoporosity of Nanoscale Mesoporous Silica on Properties of Polyimide Composite. *Macromolecules* **2006**, *39*, 7583–7590.
19. Park, S. H.; Jin, S. H.; Jun, G. H.; Hong, S. H.; Jean., S. Enhanced Electrical Properties in Carbon Nanotube/Poly (3-Hexylthiophene) Nanocomposites Formed through Non-covalent Functionalization. *Nano Res.* **2011**, *4*, 1129–1135.
20. Stankovich, S.; Dikin, D. A.; Dommett, G. H. B.; Kohlhaas, K. M.; Zimney, E. J.; Stach, E. A.; Piner, R. D.; Nguyen, S. T.; Ruoff, R. S. Graphene-Based Composite Materials. *Nature* **2006**, *442*, 282–286.
21. Park, S.; An, J.; Piner, R. D.; Jung, I.; Yang, D.; Velamakanni, A.; Nguyen., S. T.; Ruoff, R. S. Aqueous Suspension and Characterization of Chemically Modified Graphene Sheets. *Chem. Mater.* **2008**, *20*, 6592–6594.
22. Elias, D. C.; Nair, R. R.; Mohiuddin, T. M. G.; Morozov, S. V.; Blake, P.; Halsall, M. P.; Ferrari, A. C.; Boukhvalov, D. W.; Katsnelson, M. I.; Geim, A. K; *et al*. Control of Graphene's Properties by Reversible Hydrogenation: Evidence for Graphane. *Science* **2009**, *323*, 610–613.
23. Li, Y.; Hu, Y.; Zhao, Y.; Shi, G.; Deng, L.; Hou, Y.; Qu, L. An Electrochemical Avenue to Green-Luminescent Graphene Quantum Dots as Potential Electron-Acceptors for Photovoltaics. *Adv. Mater.* **2011**, *23*, 776–780.
24. Li, X.; Wang, X.; Zhang, L.; Lee, S.; Dai, H. Chemically Derived, Ultrasmooth Graphene Nanoribbon Semiconductors. *Science* **2008**, *319*, 1229–1232.
25. Sun, Y. P.; Zhou, B.; Lin, Y.; Wang, W.; Fernando, K. A. S.; Pathak, P.; Meziani, M. J.; Harruff, B. A.; Wang, X.; Wang, H.; *et al*. Quantum-Sized Carbon Dots for Bright and Colorful Photoluminescence. *J. Am. Chem. Soc.* **2006**, *128*, 7756–7757.
26. Shen, J.; Zhu, Y.; Chen, C.; Yang, X.; Li, C. Facile Preparation and Upconversion Luminescence of Graphene Quantum Dots. *Chem. Commun* **2011**, *47*, 2580–2582.
27. Morrison, R. T.; Boyd, R. N. Electrophilic Aromatic Substitution. In *Organic Chemistry*, 6th ed.; Prentice Hall International, Inc.: Upper Saddle River, NJ, 1992; p 517−546.
28. Prasad, P. N. Is There a Role for Organic Materials Chemistry in Nonlinear Optics and Photonics? *Chem. Mater.* **1990**, *2*, 660–669.
29. Osaka, T.; Mccullough, R. D. Advances in Molecular Design and Synthesis of Regioregular Polythiophenes. *Acc. Chem. Res.* **2008**, *41*, 1202–1214.
30. Loh, K. P.; Bao, Q.; Eda, G.; Chhowalla, M. Graphene Oxide as a Chemically Tunable Platform for Optical Applications. *Nat. Chem.* **2010**, *2*, 1015–1024.
31. Chien, C.-T.; Li, S.-S.; Lai, W.-J; Yeh, Y.-C.; Chen, H.-A.; Chen, I.-S.; Chen, L.-C.; Chen, K.-H.; Nemoto, T.; Isoda, S.; *et al*. Tunable Photoluminescence from Graphene Oxide. *Angew. Chem., Int. Ed.* **2012**, *51*, 6662–6666.
32. Eda, G.; Lin, Y.-Y.; Mattevi, C.; Yamaguchi, H.; Chen, H.-A.; Chen, I.-S.; Chen, C.-W.; Chhowalla, M. Blue Photoluminescence from Chemically Derived Graphene Oxide. *Adv. Mater.* **2010**, *22*, 505–509.
33. Delley, B. Fast Calculation of Electrostatics in Crystals and Large Molecules. *J. Phys. Chem.* **1996**, *100*, 6107–6110.
34. Mulliken, R. S. Electronic Population Analysis on LCAO-MO Molecular Wave Functions. *J. Chem. Phys.* **1955**, *23*, 1833–1840.